Article

Functionalization of Single-Walled Carbon Nanotubes with Well-Defined Polystyrene by "Click" Coupling

Huaming Li, Fuyong Cheng, Andy M. Duft, and Alex Adronov

J. Am. Chem. Soc., **2005**, 127 (41), 14518-14524• DOI: 10.1021/ja054958b • Publication Date (Web): 23 September 2005

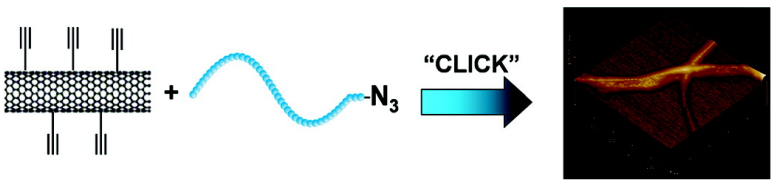

More About This Article

Additional resources and features associated with this article are available within the HTML version:

- Supporting Information
- Links to the 23 articles that cite this article, as of the time of this article download
- Access to high resolution figures
- Links to articles and content related to this article
- Copyright permission to reproduce figures and/or text from this article

View the Full Text HTML

J|A|C|S
ARTICLES
Published on Web 09/23/2005

Functionalization of Single-Walled Carbon Nanotubes with Well-Defined Polystyrene by "Click" Coupling

Huaming Li,[†] Fuyong Cheng,[†] Andy M. Duft,[‡] and Alex Adronov*[,†,‡]

Contribution from the Department of Chemistry and Brockhouse Institute for Materials Research (BIMR), McMaster University, Hamilton, Ontario L8S 4M1, Canada

Received July 23, 2005; E-mail: adronov@mcmaster.ca

Abstract: Covalent functionalization of alkyne-decorated SWNTs with well-defined, azide-terminated polystyrene polymers was accomplished by the Cu(I)-catalyzed [3 + 2] Huisgen cycloaddition. This reaction was found to be extremely efficient in producing organosoluble polymer-nanotube conjugates, even at relatively low reaction temperatures (60 °C) and short reaction times (24 h). The reaction was found to be most effective when a CuI catalyst was employed in the presence of 1,8-diazabicyclo[5.4.0]undec-7-ene as an additive. IR spectroscopy was utilized to follow the introduction and consumption of alkyne groups on the SWNTs, and Raman spectroscopy evidenced the conversion of a high proportion of sp^2 carbons to sp^3 hybridization during alkyne introduction. Thermogravimetric analysis indicated that the polymer-functionalized SWNTs consisted of 45% polymer, amounting to approximately one polymer chain for every 200−700 carbons of the nanotubes, depending on polymer molecular weight. Transmission electron microscopy and atomic force microscopy were utilized to image polymer-functionalized SWNTs, showing relatively uniform polymer coatings present on the surface of individual, debundled nanotubes.

Introduction

Due to the unique structural and electronic properties of single-walled carbon nanotubes (SWNTs),[1] they have been investigated for numerous potential applications that include molecular electronics,[2,3] sensors,[4−6] field-emission devices,[7] and components in high-performance composites.[8] Although some of these applications can be realized through in-situ growth[9,10] or solid-phase deposition of carbon nanotubes at the site of action,[10−12] many others will require solution-phase processing and manipulation to achieve appropriate assemblies, orientations, and homogeneous dispersions of carbon nanotubes within host materials.[13] Solution-phase processing, however, poses great difficulty considering the general insolubility of these structures in most organic and aqueous solvents.[14] Recently, several approaches to the functionalization of SWNTs,[15] including covalent sidewall coupling reactions,[16,17] and noncovalent exohedral interactions,[18−22] have been developed to overcome the solubility limitations. Among these approaches, covalent sidewall modification with polymeric structures has shown promise in improving the solubility of nanotube-polymer conjugates, even with a relatively low degree of functionalization.[23,24] Furthermore, the versatility of polymer chemistry allows for control over the final properties of the nanotube-polymer conjugate, which are dictated by the chemical and physical characteristics of the grafted polymer. For example, the attachment of functional polymers with controlled architectures may provide opportunities for the preparation of hybrid materials capable of environmental responsiveness and, potentially, supramolecular organization. Current methods for preparation of covalent polymer-SWNT conjugates include "grafting from" methods using initiator-functionalized SWNTs,[25−28] as well as "grafting to" methods involving radical coupling[29−32]

[†] Department of Chemistry.
[‡] Brockhouse Institute for Materials Research.

(1) Iijima, S.; Ichihashi, T. *Nature* **1993**, *363*, 603−605.
(2) Avouris, P. *Acc. Chem. Res.* **2002**, *35*, 1026−1034.
(3) Collins, P. G.; Avouris, P. *Sci. Am.* **2000**, *283*, 62−69.
(4) Dai, H. J. *Acc. Chem. Res.* **2002**, *35*, 1035−1044.
(5) Kong, J.; Franklin, N. R.; Zhou, C. W.; Chapline, M. G.; Peng, S.; Cho, K. J.; Dai, H. J. *Science* **2000**, *287*, 622−625.
(6) Kong, J.; Chapline, M. G.; Dai, H. J. *Adv. Mater.* **2001**, *13*, 1384−1386.
(7) Choi, W. B.; Chung, D. S.; Kang, J. H.; Kim, H. Y.; Jin, Y. W.; Han, I. T.; Lee, Y. H.; Jung, J. E.; Lee, N. S.; Park, G. S.; Kim, J. M. *Appl. Phys. Lett.* **1999**, *75*, 3129−3131.
(8) Ajayan, P. M. *Chem. Rev.* **1999**, *99*, 1787−1799.
(9) Wei, B. Q.; Vajtai, R.; Jung, Y.; Ward, J.; Zhang, R.; Ramanath, G.; Ajayan, P. M. *Nature* **2002**, *416*, 495−496.
(10) Dai, H. J. *Surf. Sci.* **2002**, *500*, 218−241.
(11) Rueckes, T.; Kim, K.; Joselevich, E.; Tseng, G. Y.; Cheung, C. L.; Lieber, C. M. *Science* **2000**, *289*, 94−97.
(12) Dai, L. M.; Patil, A.; Gong, X. Y.; Guo, Z. X.; Liu, L. Q.; Liu, Y.; Zhu, D. B. *ChemPhysChem* **2003**, *4*, 1150−1169.
(13) Huang, Y.; Duan, X. F.; Wei, Q. Q.; Lieber, C. M. *Science* **2001**, *291*, 630−633.
(14) Tasis, D.; Tagmatarchis, N.; Georgakilas, V.; Prato, M. *Chem.-Eur. J.* **2003**, *9*, 4001−4008.
(15) Hirsch, A. *Angew. Chem., Int. Ed.* **2002**, *41*, 1853−1859.
(16) Niyogi, S.; Hamon, M. A.; Hu, H.; Zhao, B.; Bhowmik, P.; Sen, R.; Itkis, M. E.; Haddon, R. C. *Acc. Chem. Res.* **2002**, *35*, 1105−1113.
(17) Banerjee, S.; Hemraj-Benny, T.; Wong, S. S. *Adv. Mater.* **2005**, *17*, 17−29.
(18) Nakashima, N.; Tomonari, Y.; Murakami, H. *Chem. Lett.* **2002**, 638−639.
(19) Chen, R. J.; Zhang, Y.; Wang, D.; Dai, H. *J. Am. Chem. Soc.* **2001**, *123*, 3838−3839.
(20) Chen, R. J.; Bangsaruntip, S.; Drouvalakis, K. A.; Kam, N. W. S.; Shim, M.; Li, Y. M.; Kim, W.; Utz, P. J.; Dai, H. J. *Proc. Natl. Acad. Sci. U.S.A.* **2003**, *100*, 4984−4989.
(21) Liu, L.; Wang, T. X.; Li, J. X.; Guo, Z. X.; Dai, L. M.; Zhang, D. Q.; Zhu, D. B. *Chem. Phys. Lett.* **2003**, *367*, 747−752.
(22) Gomez, F. J.; Chen, R. J.; Wang, D. W.; Waymouth, R. M.; Dai, H. J. *Chem. Commun.* **2003**, 190−191.
(23) Sun, Y. P.; Fu, K. F.; Lin, Y.; Huang, W. J. *Acc. Chem. Res.* **2002**, *35*, 1096−1104.
(24) Hill, D. E.; Lin, Y.; Rao, A. M.; Allard, L. F.; Sun, Y. P. *Macromolecules* **2002**, *35*, 9466−9471.

10.1021/ja054958b CCC: $30.25

or reaction with surface-bound carboxylic acid groups on oxidized SWNTs.[33−36] Although the "grafting from" approach promises high graft densities, attachment of initiator groups to SWNTs and control over polymer molecular weight and architecture can be difficult to achieve. Additionally, the widely used controlled radical polymerizations that have been reported to occur from nanotube surfaces may be affected by radical coupling to carbon nanotubes, potentially causing side reactions leading to decreased control over the polymerization process. Conversely, the "grafting to" approach, which involves polymer preparation prior to grafting, allows full control over polymer length and architecture, but typically results in low graft density due to steric hindrance from attached polymer chains and relatively low reactivity of functional groups on the surface of SWNTs. In addition, most of the reported nanotube grafting reactions require relatively harsh conditions, typically involving high temperatures and long reaction times. Such conditions may be incompatible with many of the functional molecules that are desirable for grafting onto SWNTs.

One potential method for achieving high graft densities while maintaining control over the polymer structure involves the application of a modular approach where SWNTs bearing a controllable number of highly reactive surface species are coupled to separately prepared, end-functionalized polymers using an efficient (preferably quantitative) coupling protocol. For such an approach to be successful, the coupling reaction would have to be relatively mild and highly selective so as to allow incorporation of various functional groups on the polymer without risk of side reactions. Recently, "click chemistry"[37] has attracted significant attention in polymer and materials science. Click reactions are attractive for carrying out polymerizations[38] as well as for modification of macromolecules[39−41] due to their modular nature, selectivity, and high yields. This allows for diverse arrays of building blocks to be prefabricated with appropriate functional groups that allow their linkage in a single convergent step. In particular, the copper(I)-catalyzed [3 + 2] Huisgen cycloaddition[42,43] has been utilized for the preparation of dendrimers,[39,44,45] dendronized polymers,[46] side-chain functional linear polymers,[47,48] and cross-linked materials.[49] It was therefore postulated that the use of click chemistry would be an ideal modular methodology for the introduction of a wide variety of molecules onto the surface of SWNTs. Here, we report the application of the Huisgen cycloaddition to the functionalization of SWNTs with polystyrene. To achieve a high degree of functionalization, we chose to introduce alkyne groups on the nanotube surface using the Pschorr-type arylation previously reported by Tour and co-workers,[50] which has been shown to modify a significant proportion of carbons within the nanotube sidewall.[51−53] Subsequent introduction of polystyrene was achieved by first installing an azide functionality at the polymer chain end. The Cu(I)-catalyzed formation of 1,2,3-triazoles by coupling azide-terminated polymer and alkyne-functionalized SWNTs was found to occur in an efficient manner under a variety of favorable conditions. This resulted in relatively high nanotube graft densities, full control over polymer molecular weight, and good solubility in organic solvents.

Results and Discussion

In these studies, pristine SWNTs prepared by the HiPco process were used without further treatment. *p*-Aminophenyl propargyl ether (**1**) was prepared by etherification of *p*-nitrophenol with propargyl bromide, followed by reduction to the corresponding aniline derivative.[54] The *p*-aminophenyl propargyl ether (**1**) was subsequently reacted with SWNTs using a solvent-free diazotization and coupling procedure[50] to produce alkyne-functionalized SWNTs **2** (Scheme 1). This chemistry allows for a high degree of functionalization and can be performed on relatively large-scale. In a typical experiment, 160 mg of SWNTs was reacted with *p*-aminophenyl propargyl ether (4 equiv/mol of carbon) in the presence of isoamyl nitrite (5 equiv/mol of carbon).

A series of well-defined polystyrene (PS) polymers was prepared by atom transfer radical polymerization (ATRP) of styrene using ethyl 2-bromoisobutyrate (EBiB) as an initiator and a CuBr/2,2′-bipyridine (BPy) complex as the catalyst. All polymerizations proceeded with good control, as evidenced by low product polydispersity (Tables 1 and 2). In addition, the ATRP reactions were stopped at approximately 60% conversion to ensure that bromine end-groups were retained. Azide terminal groups were installed on these polymers by end-group substitution with NaN_3 in DMF,[38] as depicted in Scheme 1. Complete transformation of bromo-terminated PS to azide-terminated PS was monitored using ^{1}H NMR spectroscopy, which indicated a

(25) Qin, S. H.; Oin, D. Q.; Ford, W. T.; Resasco, D. E.; Herrera, J. E. *J. Am. Chem. Soc.* **2004**, *126*, 170−176.
(26) Kong, H.; Gao, C.; Yan, D. Y. *J. Am. Chem. Soc.* **2004**, *126*, 412−413.
(27) Yao, Z.; Braidy, N.; Botton, G. A.; Adronov, A. *J. Am. Chem. Soc.* **2003**, *125*, 16015−16024.
(28) Liu, Y. Q.; Adronov, A. *Macromolecules* **2004**, *37*, 4755−4760.
(29) Lou, X. D.; Detrembleur, C.; Sciannamea, V.; Pagnoulle, C.; Jerome, R. *Polymer* **2004**, *45*, 6097−6102.
(30) Qin, S. H.; Qin, D. Q.; Ford, W. T.; Herrera, J. E.; Resasco, D. E.; Bachilo, S. M.; Weisman, R. B. *Macromolecules* **2004**, *37*, 3965−3967.
(31) Qin, S. H.; Qin, D. Q.; Ford, W. T.; Resasco, D. E.; Herrera, J. E. *Macromolecules* **2004**, *37*, 752−757.
(32) Liu, Y. Q.; Yao, Z. L.; Adronov, A. *Macromolecules* **2005**, *38*, 1172−1179.
(33) Riggs, J. E.; Guo, Z. X.; Carroll, D. L.; Sun, Y. P. *J. Am. Chem. Soc.* **2000**, *122*, 5879−5880.
(34) Sano, M.; Kamino, A.; Okamura, J.; Shinkai, S. *Langmuir* **2001**, *17*, 5125−5128.
(35) Lin, Y.; Zhou, B.; Fernando, K. A. S.; Liu, P.; Allard, L. F.; Sun, Y. P. *Macromolecules* **2003**, *36*, 7199−7204.
(36) Fernando, K. A. S.; Lin, Y.; Sun, Y. P. *Langmuir* **2004**, *20*, 4777−4778.
(37) Kolb, H. C.; Finn, M. G.; Sharpless, K. B. *Angew. Chem., Int. Ed.* **2001**, *40*, 2004−2021.
(38) Tsarevsky, N. V.; Sumerlin, B. S.; Matyjaszewski, K. *Macromolecules* **2005**, *38*, 3558−3561.
(39) Malkoch, M.; Schleicher, K.; Drockenmuller, E.; Hawker, C. J.; Russell, T. P.; Wu, P.; Fokin, V. V. *Macromolecules* **2005**, *38*, 3663−3678.
(40) Opsteen, J. A.; van Hest, J. C. M. *Chem. Commun.* **2005**, 57−59.
(41) Lutz, J. F.; Borner, H. G.; Weichenhan, K. *Macromol. Rapid Commun.* **2005**, *26*, 514−518.
(42) Rostovtsev, V. V.; Green, L. G.; Fokin, V. V.; Sharpless, K. B. *Angew. Chem., Int. Ed.* **2002**, *41*, 2596.
(43) Tornoe, C. W.; Christensen, C.; Meldal, M. *J. Org. Chem.* **2002**, *67*, 3057−3064.
(44) Wu, P.; Feldman, A. K.; Nugent, A. K.; Hawker, C. J.; Scheel, A.; Voit, B.; Pyun, J.; Frechet, J. M. J.; Sharpless, K. B.; Fokin, V. V. *Angew. Chem., Int. Ed.* **2004**, *43*, 3928−3932.
(45) Joralemon, M. J.; O'Reilly, R. K.; Matson, J. B.; Nugent, A. K.; Hawker, C. J.; Wooley, K. L. *Macromolecules* **2005**, *38*, 5436−5443.
(46) Helms, B.; Mynar, J. L.; Hawker, C. J.; Frechet, J. M. J. *J. Am. Chem. Soc.* **2004**, *126*, 15020−15021.
(47) Parrish, B.; Breitenkamp, R. B.; Emrick, T. *J. Am. Chem. Soc.* **2005**, *127*, 7404−7410.
(48) Mantovani, G.; Ladmiral, V.; Tao, L.; Haddleton, D. M. *Chem. Commun.* **2005**, 2089−2091.
(49) Diaz, D. D.; Punna, S.; Holzer, P.; McPherson, A. K.; Sharpless, K. B.; Fokin, V. V.; Finn, M. G. *J. Polym. Sci., Part A: Polym. Chem.* **2004**, *42*, 4392−4403.
(50) Dyke, C. A.; Tour, J. M. *J. Am. Chem. Soc.* **2003**, *125*, 1156−1157.
(51) Bahr, J. L.; Tour, J. M. *Chem. Mater.* **2001**, *13*, 3823−3824.
(52) Bahr, J. L.; Yang, J. P.; Kosynkin, D. V.; Bronikowski, M. J.; Smalley, R. E.; Tour, J. M. *J. Am. Chem. Soc.* **2001**, *123*, 6536−6542.
(53) Dyke, C. A.; Tour, J. M. *Chem.-Eur. J.* **2004**, *10*, 813−817.
(54) Agag, T.; Takeichi, T. *Macromolecules* **2001**, *34*, 7257−7263.

Scheme 1 [a]

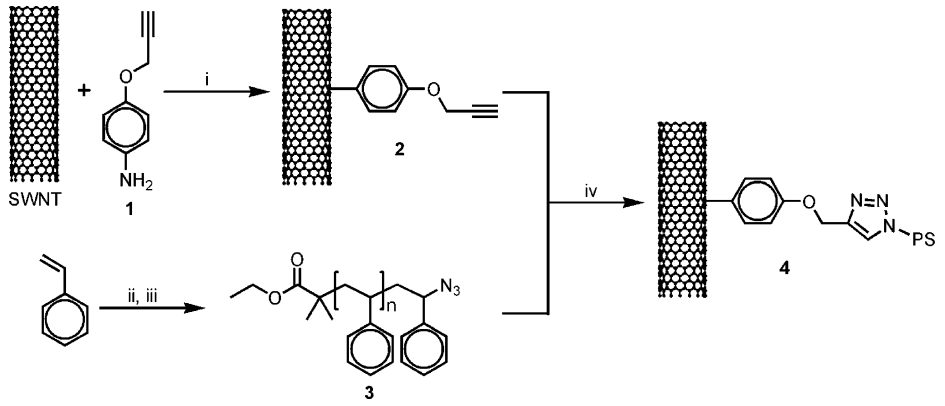

[a] (i) Isoamyl nitrite, 60 °C; (ii) EBiB, CuBr/BPy, DMF, 110 °C; (iii) NaN_3, DMF, room temperature; (iv) Cu(I), DMF.

Table 1. Results of the Polymerizations and Subsequent Coupling Reactions in DMF with $[(PPh_3)_3CuBr]$ as Catalyst

run	polymer	$M_{n,GPC}$/ kg mol^{-1}	PDI	temp/ °C	time/ h	solubility[a]/ mg L^{-1}
a	PS-N_3 [**3a**]	2.01	1.10	100	65	112
b	PS-N_3 [**3b**]	4.83	1.09	100	65	232
c	PS-N_3 [**3c**]	8.62	1.13	100	65	87
d	PS-N_3 [**3b**]	4.83	1.09	80	65	136
e	PS-N_3 [**3b**]	4.83	1.09	60	65	24
f	PS-N_3 [**3b**]	4.83	1.09	100	48	180
g	PS-N_3 [**3b**]	4.83	1.09	100	24	83

[a] The solubility of full-length polystyrene-functionalized SWNTs in THF (see Supporting Information).

Table 2. Results of the Polymerizations and Subsequent Coupling Reactions in DMF with CuI/1,8-Diazabicyclo[5.4.0]undec-7-ene (DBU) as Catalyst

run	polymer	$M_{n,GPC}$/ kg mol^{-1}	PDI	temp/ °C	time/ h	solubility[a]/ mg L^{-1}
a	PS-N_3 [**3a**]	2.01	1.10	60	24	97
b	PS-N_3 [**3b**]	4.83	1.09	60	24	233
c	PS-N_3 [**3c**]	8.62	1.13	60	24	172
d	PS-N_3 [**3b**]	4.83	1.09	90	24	226
e	PS-N_3 [**3b**]	4.83	1.09	20	48	88

[a] The solubility of full-length polystyrene-functionalized SWNTs in THF (see Supporting Information).

clear shift of the methylene protons adjacent to the end-groups from 4.4 to 3.9 ppm.

The alkyne-functionalized SWNTs (**2**) and azide-modified PS (**3**) were coupled via [3 + 2] Huisgen cycloaddition between the alkyne and azide end groups using either CuI or the organosoluble Cu(I) species, $[(PPh_3)_3CuBr]$,[44] as catalyst. All reactions were performed in DMF, yielding polymer-functionalized SWNTs (Scheme 1) as summarized in Table 1. In this study, excess PS was used in an attempt to drive the click reactions to high conversion, and this excess polymer was easily removed after each reaction by ultra-filtration and prolonged washing with THF. In addition, trace amounts of copper salts in the products were removed by washing with an aqueous ammonium hydroxide solution.

The first and simplest qualitative test to determine whether the "click" coupling procedure was successful involved checking for solubility of the product in common organic solvents. It was found that the PS-functionalized SWNTs indeed exhibited high solubility in THF, CH_2Cl_2, $CHCl_3$, and other solvents known to effectively solvate PS polymers. Conversely, any solvent in which PS does not dissolve was also incapable of dissolving

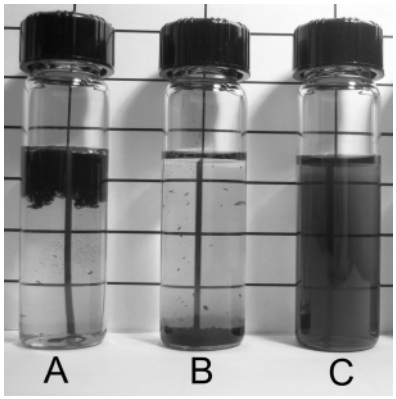

Figure 1. Photograph of three separate SWNT samples in THF. (A) Pristine SWNTs; (B) alkyne-functionalized SWNTs **2**; (C) polymer-functionalized SWNTs **4**.

the PS-SWNT conjugates. It is the polymer, therefore, that dictates the solubility properties of the overall material. Figure 1 shows three vials containing equal volumes of THF and equal masses of pristine, unmodified SWNTs (vial A), alkyne-functionalized SWNTs **2** (vial B), and the PS-SWNT conjugate **4** (vial C), where the PS number average molecular weight (M_n) is ca. 4800 g/mol. Clearly, the umodified and alkyne-functionalized SWNTs are both completely insoluble in THF (and all other common solvents), although the latter material exhibits a higher density than the former. The PS-SWNT conjugate contained in vial C forms a clear, dark-brown solution that exhibits no discernible particulate materials and remains stable for a period of at least 3 weeks. This solubility is remarkable considering that the dissolved SWNTs are, on average, greater than 1 μm in length (vide infra).

Raman spectroscopy was not only utilized to verify the structural integrity of the modified SWNT materials, but also to gather information regarding the degree of nanotube functionalization. Spectrum A in Figure 2 corresponds to pristine SWNTs, which exhibit the characteristic radial breathing ($\omega_r \approx 250$ cm^{-1}) and tangential ($\omega_t \approx 1590$ cm^{-1}) modes.[52] In addition, a weak disorder band ($\omega \approx 1290$ cm^{-1}) can be observed, indicating the presence of a small number of sp^3 hybridized carbons within the nanotube framework. Upon reaction with aniline **1**, a significant change in the disorder band was observed, in good agreement with previous studies.[50,52] Its intensity increased dramatically relative to both the radial breathing and the tangential modes, indicating that a large

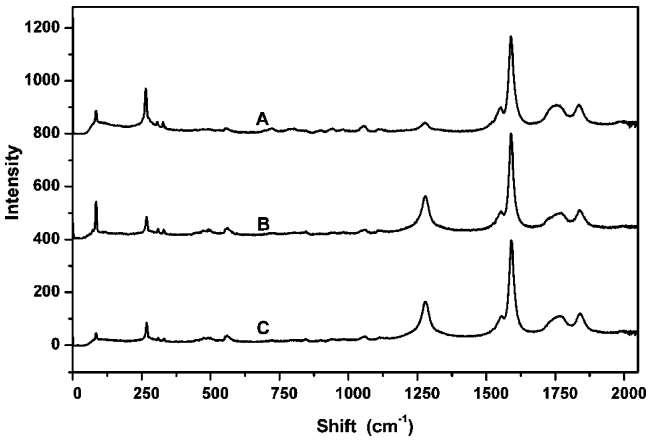

Figure 2. Raman spectra of (A) pristine SWNTs, (B) alkyne-functionalized SWNTs (**2**), and (C) polystyrene-functionalized SWNTs (**4**).

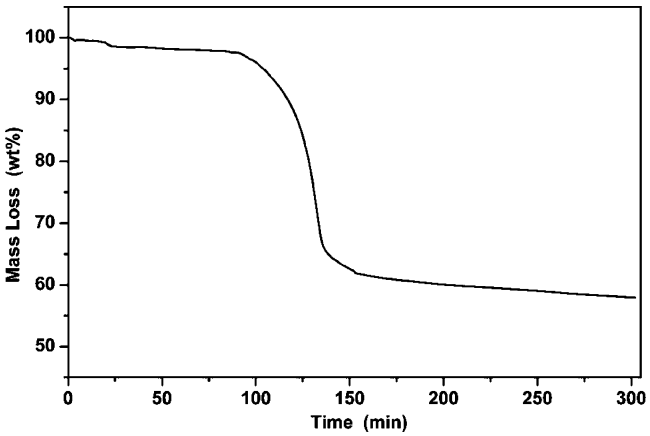

Figure 3. Thermogravimetric analysis data for polystryrene-functionalized SWNTs (**4**) having a polymer M_n = 4800 g/mol, acquired under argon. The temperature profile involved a 1 h hold at 150 °C followed by a ramp of 5 °C min^{-1} to 500 °C, and a 2.5 h hold at 500 °C.

number of sp^2 hybridized carbons have been converted to sp^3 hybridization. The intensity of the tangential mode relative to the radial breathing mode also increased, again in agreement with previous observations.[52] Upon reaction with azide-functionalized polystyrene, the intensity of the disorder band relative to the radial breathing and tangential modes remained unchanged, as would be expected because the click reaction does not alter the hybridization of carbon atoms within the nanotube framework. To gain a more quantitative picture of the extent of nanotube functionalization, thermogravimetric analysis (TGA) was performed on the reaction product (Figure 3). A mass loss of approximately 45%, due to polymer decomposition, was observed when the product was heated to 500 °C under Ar for 2.5 h. Considering the polymer molecular weight of 4800 g/mol, this mass loss corresponds to functionalization of approximately one in 500 carbon atoms on the SWNT sidewalls. The TGA experiment, when carried out using nanotubes grafted with 2000 and 8600 g/mol polymers, resulted in similar mass losses, corresponding to a functionalization of one in 200 and one in 700 nanotube carbons, respectively.

IR spectroscopy provided information about the structures appended to the surface of the SWNTs, which is not available from the Raman data. Figure 4i depicts the IR spectra of unmodified SWNTs (spectrum A), the alkyne-functionalized SWNTs **2** (spectrum B), and the polymer-functionalized SWNTs **4** (spectrum C), having a polymer molecular weight of 4800 g/mol. Clearly, the unmodified SWNTs are devoid of any identifiable functional groups, as expected (the band at ~3500 cm^{-1} corresponds to trace amounts of water present in the KBr used for preparation of the sample pellet). However, small, but clearly discernible, signals at 2120 and 3280 cm^{-1} are present in spectrum B, corresponding to the C−C and C−H stretching frequencies of the appended terminal alkyne functionalities, respectively. Additionally, signals corresponding to the C−C and C−H stretches of the aromatic ring that serves as a linker between the nanotubes and the alkyne functionality in compound **2** can be seen at 1660 and 2920 cm^{-1}, respectively. Upon cycloaddition, the IR spectrum of the product (Figure 4i, curve C) bears the characteristic signals for polystyrene,[55] indicating that polymer had been grafted. Although the alkyne signal at 2120 cm^{-1} is weak, magnification of the three spectra in the region between 2000 and 2250 cm^{-1} indicates that it is not present prior to reaction with *p*-aminophenyl propargyl ether or after the Huisgen cycloaddition (Figure 4ii). The disappearance of the alkyne stretch after the click coupling indicates that most of the alkynes must have been consumed during this reaction, although the low intensity of this IR absorption makes quantitation of conversion difficult.

The successful implementation of the click reaction on the SWNT sidewall prompted us to investigate the effect of reaction time, temperature, catalyst type, and polymer molecular weight on the solubility of the resulting SWNT-polymer conjugates. Reaction conditions were systematically varied (Tables 1 and 2), and their effect was evaluated by spectrophotometrically estimating the relative solubility of the PS-SWNT conjugates in THF. All samples were typically sonicated for 3 min and then centrifuged at 5000 rpm for 20 min, followed by standing undisturbed overnight prior to UV/vis absorption measurements, which were performed on the supernatant of the resulting sample. A previously determined specific extinction coefficient of 0.0103 L mg^{-1} cm^{-1} was used to estimate the nanotube concentrations.[32] We first determined the effect of polymer molecular weight, reaction time, and temperature using the organosoluble Cu(I) species, $[(PPh_3)_3CuBr]$,[44] as the catalyst (all cycloaddition reactions were performed in DMF). Comparing entries a, b, and c of Table 1 provides an indication that polymer molecular weight has an impact on the solubility of the conjugate materials. Interestingly, at a molecular weight of 4800 g/mol, corresponding to approximately 50 styrene repeat units, the polymer imparts the highest solubility at 233 mg/L. When the molecular weight is decreased to ~2000 g/mol, the solubility drops by a factor of 2. This is likely due to a decreased polymer−solvent interaction that diminishes the solubilizing strength of the polymer at lower molecular weight. Alternatively, when the molecular weight is incleased to ~8600 g/mol, the conjugate solubility also dropped. This result can be explained by the decreased reactivity of the chain-end azide functionality that becomes less accessible as the polymer adopts a more random coil structure at this higher molecular weight. Therefore, as the polymer molecular weight is increased, the polymer graft density decreases, as also indicated by TGA. Clearly, a balance between end-group accessibility and polymer solubilizing

(55) Silverstein, R. M.; Webster, F. X. *Spectrometric Identification of Organic Compounds*, 6th ed.; John Wiley & Sons: New York, 1998.

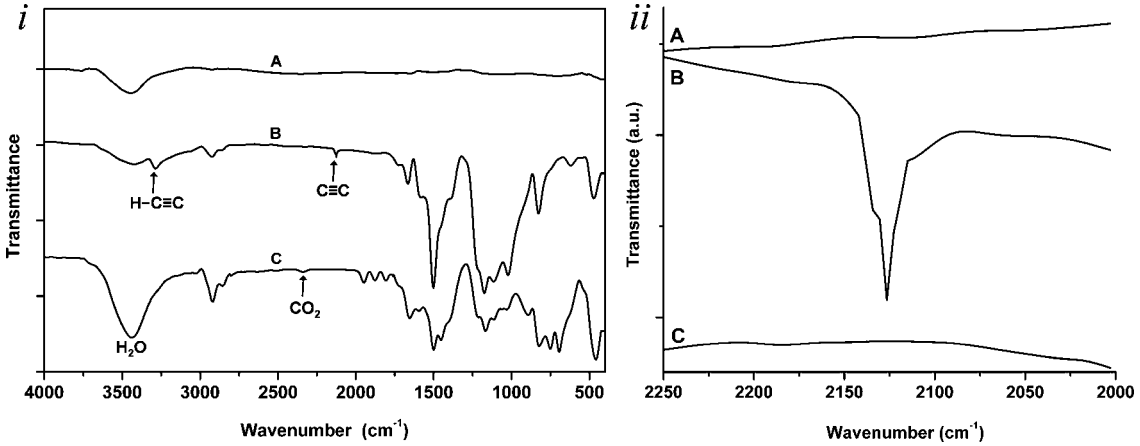

Figure 4. (i) IR spectra of (A) pristine SWNTs, (B) alkyne-functionalized SWNTs, and (C) polystyrene-functionalized SWNTs. (ii) Expanded region between 2000 and 2250 cm^{-1} of the same three samples, highlighting the appearance and disappearance of the alkyne stretch at 2120 cm^{-1}.

strength must be reached to maximize solubility of the conjugates.

Comparing entries b, d, and e (Table 1) provides information on the effect of reaction temperature on solubility of the final product. Using this catalyst system, it appears that higher temperatures improve the efficiency of the cycloaddition reaction. The effect of time can also be gleaned from entries b, f, and g, indicating that longer reaction times improve solubility, but this improvement diminishes beyond reaction times of 48 h.

In an attempt to decrease reaction time and temperature, while maintaining a high conjugate solubility, the catalyst system was changed to CuI with 1,8-diazabicyclo[5.4.0]undec-7-ene (DBU) as an additive. This combination was previously reported by Gin and co-workers as an effective combination for the Huisgen cycloaddition.[56] Using this catalyst system, it was possible to achieve solubilities comparable to the ones with $[(PPh_3)_3CuBr]$, but at a reaction temperature of 60 °C after only 24 h (Table 2, entry b). Longer reaction times under these conditions did not lead to improved solubility. Again, it was found that the highest solubility was achieved with the 4800 g/mol polymer (compare entries a, b, and c of Table 2). Increasing the reaction temperature to 90 °C resulted in no improvement of solubility (entry d), while decreasing to 20 °C lowered the solubility significantly, even when reaction time was doubled. It should be noted that using the CuI/DBU system resulted in greater solubility at a temperature of 20 °C than what was achieved with the $[(Ph_3P)_3CuBr]$ at 60 °C (compare entry e from Tables 1 and 2). In all of these experiments, deoxygenation of the reagent mixture at the beginning of each reaction was critical to maintaining an active Cu(I) catalyst throughout the cycloaddition. All mixtures were therefore evacuated and refilled with N_2 at least three times to remove oxygen before commencing the reaction.

Interestingly, the SWNTs that were functionalized with 8600 g/mol PS tended to precipitate from solution over 24 h. However, the precipitated material (in the form of a fine black powder) could be redispersed to form a completely homogeneous solution by simply shaking the mixture for a few seconds, without the need for sonication (see Supporting Information). Such materials may have applications in solid-phase synthesis or recycling homogeneous catalysts, where nanotube bound reagents or catalysts are kept in homogeneous solution while stirring, but precipitate when stirring is stopped at the end of the reaction.

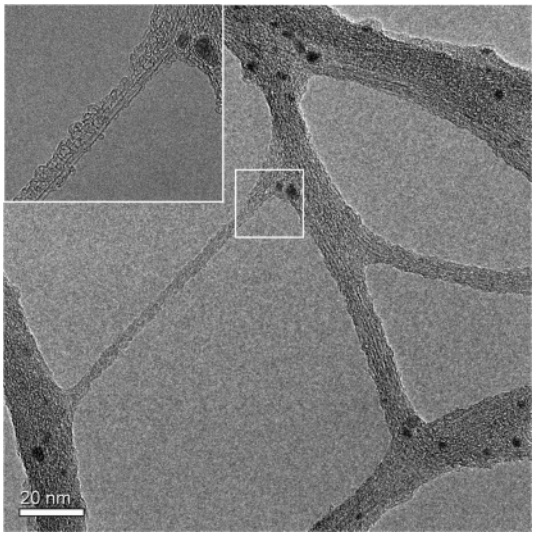

Figure 5. TEM image of polystyrene-functionalized SWNTs (inset is a magnified version of the area within the white square).

Recently, Ford and co-workers reported the direct cycloaddition of azide-terminated PS to unmodified SWNTs via nitrene formation upon thermolysis of the terminal azide group.[31] This chemistry was carried out in 1,2-dichlorobenzene at 130 °C under a nitrogen atmosphere, with a reaction time of 60 h. As a control experiment, we attempted coupling our azide-terminated PS to as-received, unmodified SWNTs. We found that stirring a mixture of polymer, SWNTs, and either of the Cu(I) catalysts in DMF at 100 °C for 90 h led to reaction products that exhibited no solubility. We can therefore rule out any direct nitrene coupling through the thermolysis of the azide-terminated PS under our reaction conditions.

High-resolution transmission electron microscopy (TEM) analysis of the PS-SWNT conjugates was performed by placing a single drop of the THF solution onto a holey carbon-coated copper grid. Figure 5 depicts representative features showing interconnected fiberlike structures composed largely of amorphous carbon in which the characteristic striations indicative of individual, embedded SWNTs are observed. The inset of

(56) Bodine, K. D.; Gin, D. Y.; Gin, M. S. *J. Am. Chem. Soc.* **2004**, *126*, 1638−1639.

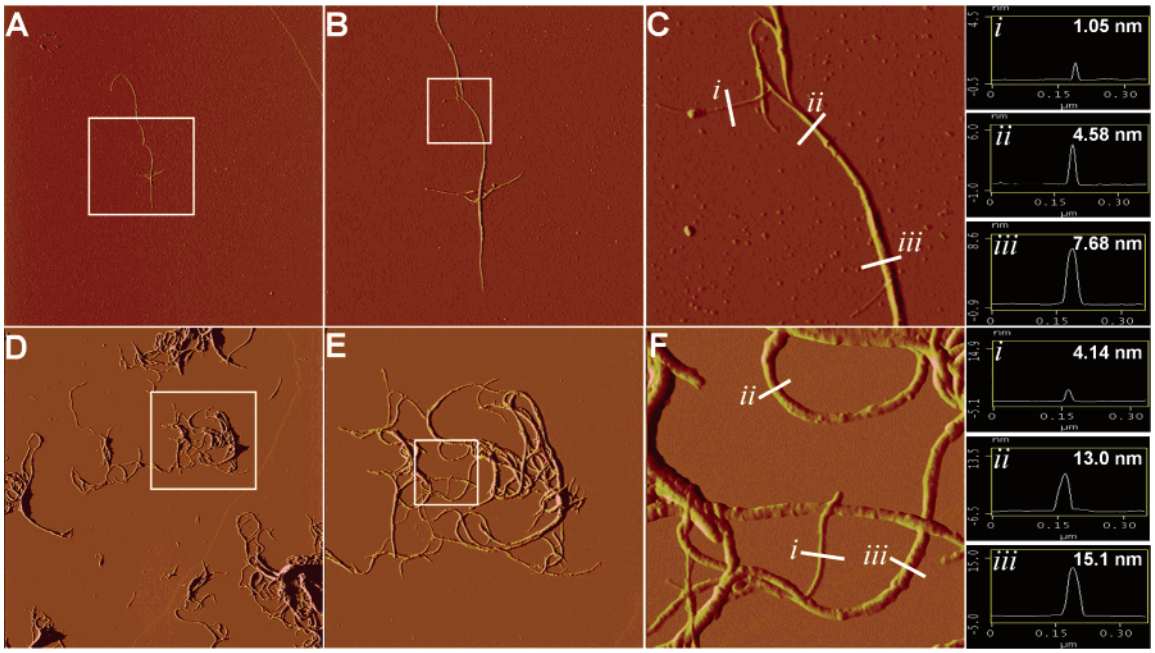

Figure 6. AFM images of pristine SWNTs (A−C) and polystyrene-functionalized SWNTs (D−F), with height profiles of different sections of images C and F given on the right. Total scales of images vary from 15 μm (A and D) to 5 μm (B and E) and to 1 μm (C and F).

Figure 5 shows a particularly well-resolved feature in which two or three individual polymer-coated SWNTs can be seen. The presence of such individual SWNTs is indicative of debundling of SWNTs as a result of polymer functionalization.

To complement the TEM data, atomic force microscopy (AFM) was also performed. Figure 6 consists of two sets of AFM images that represent the pristine SWNTs (images A−C) and the 4800 g/mol PS-functionalized SWNTs **4** (images D−F). In each set, the magnification increases such that the image scale totals 15, 5, and 1 μm on going from left to right (magnified sections of images A, B, D, and E are indicated by a white box). The height profiles for the three marked sections of each 1 μm^2 image are given on the right. The two samples were prepared by spin-coating THF suspensions onto freshly cleaved mica at 2500 rpm. Due to the lack of solubility of the unmodified SWNTs, this compound required several minutes of sonication immediately prior to the spin-coating procedure. Conversely, the polymer-functionalized material was used after centrifugation and standing (vide supra) and required no sonication as it remained in the form of a stable solution for a period of at least 3 weeks. Comparing the lowest magnification images, it can be observed that the unmodified SWNTs result in very few individually dispersed features (image A) that were relatively difficult to find, with most of the sample forming large aggregates that were not imageable without damaging the AFM tip. However, the polymer-functionalized material leads to numerous easily measurable nanotube-based features in every 15 × 15 μm spot that was imaged. Comparing images C and F, a clear difference due to polymer functionalization can be observed. The polymer-functionalized material exhibits nanotube strands that are thicker than the original SWNT bundles. Although most of the material in image C resides in bundles that are 4−7 nm in height, some individual tubes with heights around 1 nm are observable. Upon functionalization, the isolated soluble material exhibits individual nanotube strands that have a relatively uniform polymer coating, with a minimum height of approximately 4 nm. In this case, multiple strands still aggregate into thicker "ropes" exhibiting height profiles of ca. 15 nm. It is likely that the thicker nanotube ropes consist of individual polymer-functionalized SWNTs that have become associated with one another during the spin-coating process, rather than bundles of SWNTs that are polymer-functionalized only on their exterior. The polymer functionalization process must therefore cause alkyne-functionalized SWNT bundles to exfoliate, resulting in the formation of individual polymer-coated nanotubes in solution. This is supported by the observation of numerous features corresponding to ropes splitting into several smaller polymer-coated strands as well as regions where one strand passes between two strands of a separate rope (Figure 7). The observed high solubility of these structures, as well as their long-term stability in solution (even during high-speed centrifugation), are also consistent with individual nanotubes, rather than larger bundles, having been grafted with polymer.

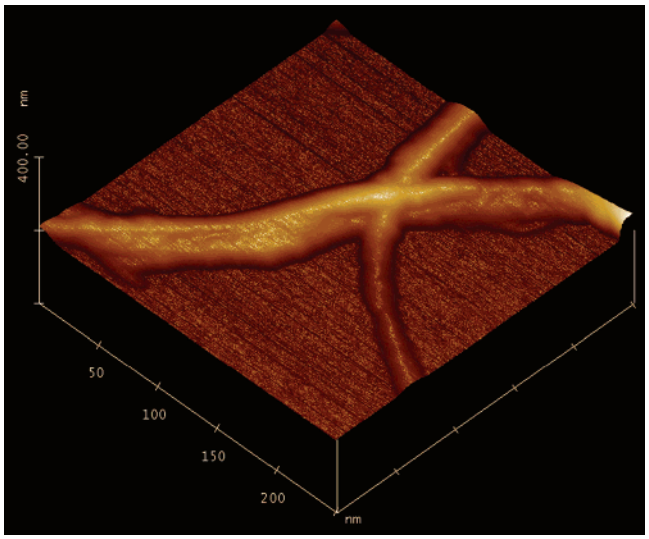

Figure 7. AFM surface plot of a PS-SWNT strand passing through a separate multi-nanotube rope.

Conclusion

We have demonstrated a highly efficient, modular approach to the functionalization of SWNTs with polystyrene using the Cu(I)-catalyzed [3 + 2] Huisgen cycloaddition. The separate preparation of alkyne-functionalized SWNTs and azide-terminated polymers allowed for characterization of both materials prior to the convergent grafting step. A number of reaction parameters were investigated, allowing the identification of relatively mild coupling conditions, using CuI/DBU as the catalyst system. TGA of the PS-SWNT conjugates indicated a grafting density of 1 polymer chain for every 200−700 nanotube carbons, resulting in a material that consisted of approximately 45% polymer. These materials exhibited high solubility in organic solvents such as THF, $CHCl_3$, and CH_2Cl_2. TEM and AFM analysis clearly showed the presence of polymer-coated SWNTs in solutions that remained stable for at least 3 weeks. Currently, we are extending this approach to the functionalization of SWNTs with other polymeric and functional materials.

Acknowledgment. We would like to thank Fred Pearson for help with TEM measurements and Frank Gibbs for TGA data. Financial support for this work was provided by the Natural Science and Engineering Research Council of Canada (NSERC) Strategic Grants program, the Canada Foundation for Innovation (CFI), the Ontario Innovation Trust (OIT), and the Materials and Manufacturing Ontario Emerging Materials Knowledge Fund (EMK). H.L. would also like to gratefully acknowledge the China Scholarship Council for financial support in the form of a fellowship for international study.

Supporting Information Available: Full experimental details for all compounds, as well as a video clip showing dissolution of polymer-functionalized SWNTs upon shaking. This material is available free of charge via the Internet at http://pubs.acs.org.

JA054958B